Extended Abstracts of the 2007 International Conference on Solid State Devices and Materials, Tsukuba, 2007, pp. 360-361

P-1-19

UV-VIS Raman Characterization of High Dose Ultra Shallow Implanted Silicon before and after Excessive Annealing

T. Sasaki[1*], H. Minami[1], K. Kisoda[2], W. S. Yoo[3], M. Yoshimoto[1] and H. Harima[1]

[1]Kyoto Institute of Technology, Matsugasaki, Kyoto 606-8585, Japan,
Phone: +81-75-724-7421 [*]E-mail: m6621021@edu.kit.ac.jp
[2]Wakayama University, Wakayama 640-8510, Japan
[3]WaferMasters, Inc., San Jose, California, 95112, U.S.A.

1. Introduction

Formation of ultra shallow junctions is a key issue in reducing dimensions of modern Si chip elements. For this purpose, ion implantation with ultra shallow projected range of less than ~10 nm in depth is required, as well as a novel annealing technique for dopant activation with minimum diffusion. Needless to say, such technology cannot be developed without precise characterization of the processed region.

Raman spectroscopy using UV lasers for excitation (UV-Raman) is an ideal tool for characterizing surface and sub-surface regions because the laser penetration depth is typically less than 10 nm in Si [1]. In this study, a shallow-implanted Si wafer is characterized by Raman scattering using UV and visible lasers for excitation (UV-VIS Raman). Variation of crystallinity with depth is analyzed using different penetration depths of probe lasers.

2. Experiment

Boron ions were implanted into an n-type Si (100) wafer at acceleration voltage of 1 keV with dose $2x10^{15}$ cm^{-2}. The wafer was then excessively annealed for intentional boron diffusion by a pulsed, focused laser annealing system at different powers, termed annealing A (low power) and B (higher power).

The effects of annealing on the crystal quality of the sample was observed by microscopic Raman scattering with UV lasers at wavelength λ_{ex}=266.0 and 363.8 nm, and visible region lasers at 457.9, 488.0 and 514.5 nm. The laser penetration depth δ (=1/α, with α being the absorption coefficient) is approximately equal to 5, 10, 280, 480, 660 nm, respectively, and has the following meaning: when back-scattered photons are observed (see Fig.1 for the setup), about 90% of the signal emanates from the surface region within depth, δ. We also evaluated the depth profile of boron concentration by secondary ion mass spectroscopy (SIMS) for reference.

3. Results

To get an idea of the boron distribution with depth, SIMS data is shown in Figs.2(b) and 2(c) along with a scale of the laser penetration depths used in the Raman probing, Fig.2(a), in both logarithmic and linear scales. Boron was first confined in the implanted surface region with depth <10 nm with peak concentration [B]=$2x10^{21}$ cm^{-3}. Then, its distribution was flattened by diffusion with annealing to a depth d_D~150 nm with [B]~$1x10^{20}$ cm^{-3} (low power annealing A), or d_D~250 nm with ~0.5 $x10^{20}$ cm^{-3} (higher power annealing B).

In Fig.3(a), Raman spectra of the as-implanted sample for λ_{ex}=266.0 through 514.5 nm, along with a reference sample (Si wafer before implantation for λ_{ex}=514.5 nm) are shown from top to bottom for comparison. The reference gives a sharp phonon peak at 520.3 cm^{-1} with width (FWHM) 3 cm^{-1}. The top spectrum for λ_{ex}=266.0 nm shows, however, a distinctly different feature consisting of at least two broad peaks. The component peaked at ~480 cm^{-1} (A) is derived from the "signature" of amorphous silicon (a-Si) from ion-implant damage [2]: The absence of long-range lattice ordering breaks the *q*-selection rule of Raman scattering, to yield a broad peak resembling a Si-phonon density of states. Such a signal is also commonly observed in low-temperature deposited films of Si [3]. The other component (B) at ~510 cm^{-1} is derived from damaged Si. Raman helps us "observe" the crystal quality and structures non-destructively. According to reported simulations [2,3], the defect-free crystallites have dimensions of ~3 nm. For λ_{ex}=363.8 nm, on the contrary, only a sharp peak appears as in the case of the visible lasers. [See Fig.4(a), where the frequency and width of the crystalline peak are plotted against λ_{ex}]. Recalling the small difference in δ between λ_{ex}=266.0 and 363.8 nm (δ=5 and 10 nm, respectively), this drastic spectral difference clearly reveals a very abrupt variation in crystallinity. The as-implanted surface region is heavily damaged within a depth of 5 nm, but is almost damage-free between 5 and 10 nm. It is not surprising that the spectrum for λ_{ex}=363.8 nm is dominated by the crystalline signal, because crystals give much higher Raman scattering efficiency than the amorphous formation. The visible lasers, having much larger δ than the implant range are, of course, dominated by the crystalline signal.

In the top of Fig.3(b), for λ_{ex}=266.0 nm, the a-Si signal (A) is weak compared to that in Fig.3(a), while the crystalline signal (B) is slightly sharpened and peak-shifted to higher frequency [Fig.4(b)]. This is due to recrystallization caused by annealing [2,3]. The crystalline peak (B) for λ_{ex}=363.8 nm is broadened, similar to λ_{ex}=266.0 nm, due to the boron diffusion-induced lattice disordering in the probed region. Penetration depth, δ, for the visible lasers are much larger than the diffused region (d_D~150 nm), and thus cannot effectively probe the disordered region. When the sample was annealed at higher power (anneal B), [Fig.3(c)], the diffused region (d_D~250 nm) is now close to δ for λ_{ex}=457.9 nm (δ =280nm).

Therefore, we see the peak is broadened and frequency-shifted from the crystalline peak in this disordered region [Fig.4(c)]. The peak width and frequency show a systematic variation from λ_{ex}=266.0 to 457.9 nm, reflecting gradation in lattice disordering.

4. Conclusion

We have shown that UV Raman spectroscopy is a convenient tool to give insight into the lattice condition in the nm-regime below the Si surface following ion implantation and recovery by annealing.

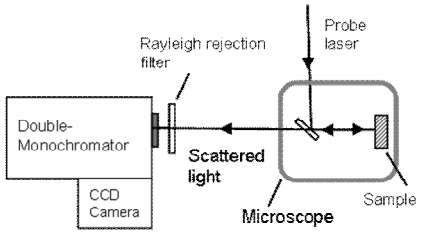

Fig.1 Raman scattering setup

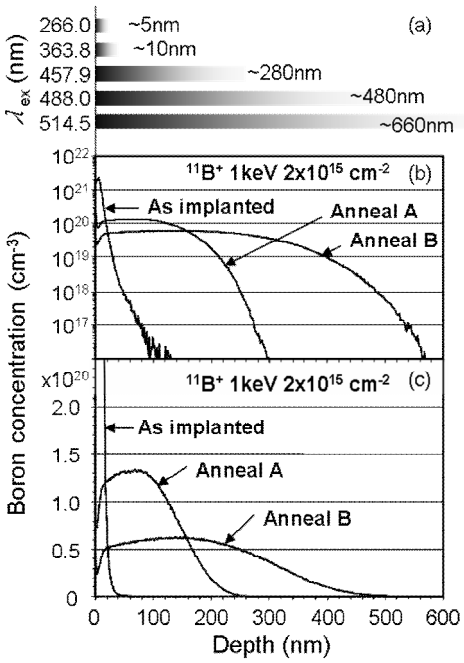

Fig.2 Laser penetration depth (a) and SIMS depth profile of boron in logarithmic (b) and linear scale (c).

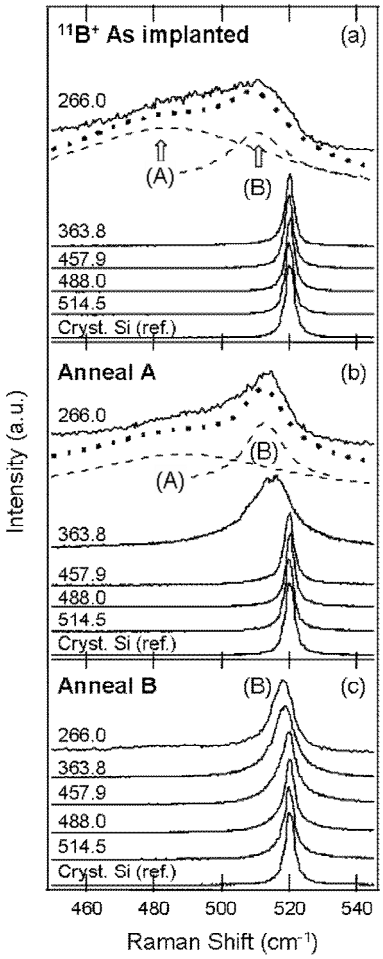

Fig.3 Raman spectra of as-implanted Si (a), and after annealing A (b) and B (c) for five different excitation laser wavelengths (nm).

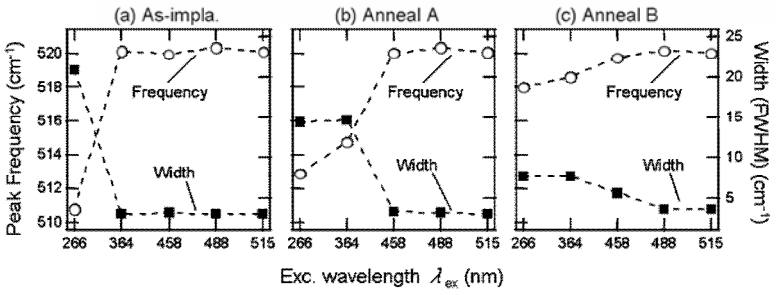

Fig.4 Peak frequency and width of crystalline peak versus excitation laser wavelength.

References

[1] M.Yoshimoto, H.Nishigaki, H.Harima, T.Isshiki, K.Kang and W.S.Yoo, *J. Electrochem .Soc.* **153** G679 (2006).

[2] G. Viera, S. Huet, E. Bertran and L. Boufendi, *J. Appl. Phys.* **90** 4272 (2001).

[3] Z.Iqbal and S.Veprek, *J. Phys.C: Solid State Phys.* **15** 377 (1982).